Article type: Primary Research Articles

Running head: Recent boreal peatland-climate feedback

Decreased carbon accumulation feedback driven by climate-induced drying of two southern boreal bogs over recent centuries

Hui Zhang[1,2,3*], Minna Väliranta[2,3], Sanna Piilo[2,3], Matthew J. Amesbury[2,4], Marco A. Aquino-López[5], Thomas P. Roland[4], Susanna Salminen-Paatero[6], Jussi Paatero[7], Annalea Lohila[1,7], Eeva-Stiina Tuittila[8]

[1]Institute for Atmospheric and Earth System Research (INAR), Department of Physics, P.O. Box 68 (Pietari Kalmin katu 5), University of Helsinki, Helsinki, Finland

[2]Environmental Change Research Unit (ECRU), Ecosystems and Environment Research Programme, University of Helsinki, Helsinki, Finland

[3]Helsinki Institute of Sustainability Science (HELSUS), Helsinki, Finland

[4]Geography, College of Life and Environmental Sciences, University of Exeter, Exeter, UK

[5]Arts and Humanities Institute, Maynooth University, Maynooth, Ireland

[6]Department of Chemistry, Radiochemistry, University of Helsinki, Helsinki, Finland

[7]Finnish Meteorological Institute, Helsinki, Finland

[8]School of Forest Sciences, University of Eastern Finland, Joensuu, Finland

[*]Correspondence to: Hui Zhang, +358413690427, hui.zhang@helsinki.fi

Hui Zhang: ORCID: 0000-0002-3758-5722,

Keywords:

Peatland community shifts, drying, carbon accumulation, boreal bogs, global warming

Abstract

Northern boreal peatlands are important ecosystems in modulating global biogeochemical cycles, yet their biological communities and related carbon dynamics are highly sensitive to changes in climate. Despite this, the strength and recent direction of these feedbacks are still unclear. The response of boreal peatlands to climate warming has received relatively little attention compared with other northern peatland types, despite forming a large northern hemisphere-wide ecosystem. Here we studied the response of two ombrotrophic boreal peatlands to climate variability over the last *c*. 200 years for which local meteorological data are available. We used remains from plants and testate amoebae to study historical changes in peatland biological communities. These data were supplemented by peat property (bulk density, carbon and nitrogen content), ^{14}C, ^{210}Pb and ^{137}Cs analyses and were used to infer changes in peatland hydrology and carbon dynamics. In total, six peat cores, three per study site, were studied that represent different microhabitats: low hummock, high lawn and low lawn. The data show a consistent drying trend over recent centuries, represented mainly as a change from wet habitat *Sphagnum* spp. to dry habitat *S. fuscum*. Summer temperature and precipitation appeared to be important drivers shaping peatland community and surface moisture conditions. Data from the driest microhabitat studied, low hummock, revealed a clear and strong negative linear correlation ($R^2 = 0.5031$, $p < 0.001$) between carbon accumulation rate and peat surface moisture conditions: under dry conditions, less carbon was accumulated. This suggests that at the dry end of the moisture gradient, availability of water regulates carbon accumulation. It can be further linked to the decreased abundance of mixotrophic testate amoebae under drier conditions ($R^2 = 0.4207$, $p < 0.001$). Our study implies that if effective precipitation decreases in the future, the carbon uptake capacity of boreal bogs may be threatened.

Introduction

Peatlands play a key role in global biogeochemical cycling by fixing atmospheric CO_2 through plant photosynthesis and releasing CO_2 and CH_4 through decomposition. Peatland biological communities (plants and microbes) are strongly controlled by temperature and hydrology, which affect peatland carbon (C) sequestration and sink potential (Jassey et al., 2015; Laine et al., 2019; McPartland et al., 2019; Riutta et al., 2007). Bog plant communities dominated by Sphagna are sensitive to environmental change, especially during the growing season (Loisel, Gallego-Sala, & Yu, 2012), and plant functional type successions may even occur under climate change, which could impact peatland carbon sink capacity (Loisel et al., 2014). Likewise, testate amoebae, the dominant group of protozoa in peatlands, play an important role in nutrient and carbon cycling (Gilbert, Amblard, Bourdier, & Francez, 1998). In particular, mixotrophic testate amoebae (MTA), which partly rely on photosynthesis, contribute to carbon sequestration in *Sphagnum* peatlands (Lara and Gomaa, 2017). Due to their sensitivity to hydrology (Charman, Hendon, & Woodland, 2000), climate change may alter the abundance of mixotrophic testate amoebae in *Sphagnum* peatlands, and thus carbon uptake. Despite their small size and biomass, it has been shown that a 50% decrease in the biomass of MTA can be linked to a significant reduction of net C uptake (-13%) of the entire *Sphagnum* bryosphere (Jassey et al., 2015).

Whilst global scale warming is projected to continue, precipitation patterns remain more regionally variable (Collins et al., 2013). The climate model intercomparison project (CMIP5) under an RCP8.5 scenario predicts warmer and wetter climate for Fennoscandia (Collins et al., 2013). However, these predictions cannot be directly applied to infer peatland hydrological

conditions, which are ecohydrologically complex due to the synchronous forcing of precipitation, evapotranspiration and runoff (Wu, Kutzbach, Jager, Wille, & Wilmking, 2010; Zhang et al., 2018a), supplemented by autogenically-driven successional processes (Tuittila, Väliranta, Laine, & Korhola, 2007).

Millennial-scale peat proxy studies from southern Finland have shown dynamic community variations, with variations both between plant functional types and within *Sphagnum* spp. (Tuittila et al., 2007; Väliranta et al., 2007, 2012). However, to date, there is a lack of studies on more recent peatland dynamics in southern Finland and their response to recent climate change, such as post Little Ice Age (LIA; *ca*. AD 1400-1850) warming or human-induced warming since the late 1900s. Tree ring-based climate reconstructions (Helama et al., 2014) and instrumental measurements from southern Finland suggest a clear increase in summer temperatures since the LIA, with cooler and wetter summers during the LIA giving way to increasingly warmer summer temperatures towards the end of the 20th century (Helama, Meriläinen, & Tuomenvirta, 2009; Luoto & Helama, 2010). Experimental studies applying open top chambers or mesocosms that started in the 2000s provide empirical short-term simulation data of peatland responses to different climate conditions (Dieleman, Branfireun, McLaughlin, & Lindo, 2015; Mäkiranta et al., 2018; Ward et al., 2013; Weltzin, Bridgham, Pastor, Chen, & Harth, 2003; Wiedermann, Nordin, Gunnarsson, Nilsson, & Ericson, 2007). A very recent experimental study of plant community response to a 15 year-long water-table drawdown suggested that fen vegetation is less resilient to water level changes, with these communities experiencing clear species turnover, while bog vegetation appeared to be more resistant (Kokkonen et al., 2019). Considering this potentially slower response time of bog vegetation to changes in the environment, there is a need for studies which capture longer time

periods than allowed by field experiments. Aerial photographs offer decadal-scale opportunity to observe changes in peatland environments but mainly at a landscape scale (Jauhiainen, Holopainen, & Rasinmäki, 2007; Tahvanainen, 2011). Only the most modern remote sensing techniques are accurate enough to investigate small-scale changes in vegetation type composition (e.g., vascular plants, mosses) over a few decades (Mikola et al., 2018). Proxy-based analysis of peat profiles has the potential to provide accurate and long-term perspectives on peatland dynamics over centuries, but so far, in the boreal climate zone it has only been recently applied to permafrost peatlands in western Canada (Magnan et al., 2018; Piilo et al., 2019; van Bellen et al., 2018). In short, there is a clear gap in understanding the responses and feedbacks of boreal bogs to on-going warming over timescales (i.e. decadal to centennial) relevant to contemporary and future climate and environmental change scenarios.

The links between vegetation, moisture conditions and climate are vital in understanding past, and in modelling future, peatland carbon dynamics (Frolking et al., 2010; Strack, Waddington, Rochefort, & Tuittila, 2006). Currently, large uncertainties remain in models of peatland dynamics due to a lack of quantitative understanding on peatland vegetation successions on decadal to centennial time scales. This study aims to quantifiably test whether changes in plant and testate amoeba communities, as well as carbon accumulation, are related to local climate variation over the past 200-300 years – a period that captures both post-LIA and post-industrial climate warming. More specifically, we aim to 1) reconstruct changes in peatland vegetation, hydrology and carbon dynamics over the past 200–300 years; 2) link the detected changes in peatland dynamics to measured climate parameters, namely summer temperature and precipitation; 3) determine the vegetation-hydroclimate-carbon dynamic feedbacks in boreal peatlands. To address the microtopographically heterogeneous nature of bogs, we examined

three different microhabitats at each study site. This experimental design enabled habitat-to-habitat and site-to-site comparisons and provides the first high-resolution centennial-scale multiproxy study for northern boreal bogs in which replicated ^{210}Pb and ^{14}C-dated peat records encompassing different microhabitats are presented.

Material and methods

Study sites and sampling

The two study sites, Siikaneva (61.83650°N, 24.17262° E) and Lakkasuo (61.78625° N, 24.30908° E), are located in southern Finland (Figure 1), *c*. 6 km from one another and in separate hydrological catchments. Based on the 30-year averages (1981–2010) from the nearest weather station, Juupajoki-Hyytiälä (61.8456° N, 24°2906 E), the mean annual temperature of the area is 4.2 °C and mean annual precipitation is 711 mm (Pirinen et al., 2012).

The Siikaneva peatland complex, which is surrounded mainly by boreal forest (Figure 1a), contains both fen and bog areas. The studied peat cores were collected within the bog area, which hosts a well-pronounced microtopography represented by open-water pools, bare peat surfaces, hollows and higher and drier lawns and hummocks (Korrensalo et al., 2018). The bog surface is covered by *Sphagnum* mosses, except in the ponds and bare peat surfaces. *Sphagnum fuscum* and *S. rubellum* grow on hummocks, where vascular plant vegetation is dominated by dwarf shrubs, such as *Andromeda polifolia*, *Calluna vulgaris* and *Empetrum nigrum*. *Eriophorum vaginatum* is also found on hummocks and is common on lawns, where the moss layer is dominated by *S. magellanicum* and *S. rubellum*. Wet hollows are dominated by *S.*

cuspidatum and *S. majus*, *Carex limosa*, *Rhynchospora alba* and *Scheuchzeria palustris*.

Lakkasuo peatland is an eccentric raised peatland complex surrounded by boreal forests (Figure 1b). The sampled bog area is a mosaic of ecohydrological gradients from dry hummocks, to intermediate lawns and wet hollows (Andersen et al., 2011). The habitat-specific vegetation features are similar to those at Siikaneva.

Samples were collected in October 2016 using a 60-cm long box corer from the transition zone between hummock and hollow, the extreme ends of moisture gradient, because the transition zone is most sensitive to changing environmental conditions (De Vleeschouwer, Chambers, & Swindles, 2010). At each site, we collected three peat cores along a moisture gradient within the transition zone: from low hummock (LH), high lawn (HL) and low lawn (LL) (Figure 1c, Table 1). Water-table depth (WTD, cm) at each sampling point was measured and dominant vegetation of the coring point was surveyed (Table 1). Individual cores were wrapped in plastic and transported to the laboratory in sealed PVC tubes and stored in a freezer. The cores were later defrosted and sub-sampled in 1-cm thick slices for further analyses. In addition, a survey of surface vegetation and WTD (measured over the 2016 growing season) was also carried out at both sites. In total, 19 plots were investigated, covering the main variations in vegetation.

Chronology

Radiocarbon (^{14}C), lead (^{210}Pb) and caesium (^{137}Cs) dating methods were used to establish the chronologies. In total, six basal bulk peat samples, which represent equally good dating materials as picked plant remains, especially for *Sphagnum* bogs (Holmquist et al., 2016), were

sent to Poznan Radiocarbon Laboratory (Poznan, Poland) for ^{14}C dating. Roots and rootlets were picked out and discarded to avoid contamination. The chemical pre-treatment followed the standard acid-base acid method for peat samples (coded as WW) (Brock, Higham, Ditchfield, & Ramsey, 2010). The chronology of the top part of each core (*c*. 40 cm) was determined primarily with ^{210}Pb dating. The ^{210}Pb dating samples were treated at the University of Exeter, UK (cores SLH, SHL, LLH and LHL) and University of Helsinki, Finland (cores SLL and LLL). A dry *c.* 0.2-0.5 g subsample from each 1-cm or 2-cm interval was analysed for ^{210}Pb activity after spiking with a ^{209}Po yield tracer; see Kelly et al. (2017) and Estop-Aragonés et al. (2018) for detailed procedure. The alpha spectrometry counting was conducted at the University of Exeter for all the cores. Additionally, caesium (^{137}Cs) dating with γ spectrometry, which provides date "markers", was applied on single core SLH at the Finnish Meteorological Institute to validate the ^{210}Pb results (Arnaud et al., 2006; Jeter 2000). The ^{137}Cs-peak, indicating 1986 AD (when the Chernobyl disaster occurred), was used as a date maker and integrated into the age-depth model of SLH.

Age-depth models were developed using *Plum* (Aquino-López et al., 2018) in R version 3.6.0 (R Core Team, 2019). ^{14}C ages were calibrated using the IntCal13 calibration curve (Reimer et al., 2013). Total ^{210}Pb data (Bq/Kg) were inputted in *Plum* and the number of samples which *Plum* used was determined by the pre-analysis within the software with exception of those cases where equilibrium was reached in the three or less deepest samples (LLH, LHL, SHL and SLL). *Plum* is capable of integrating ^{210}Pb and radiocarbon dates into a single chronology by avoiding remodelling of the ^{210}Pb, resulting in an unbiased chronology. This study represents the first application of *Plum* that integrates both ^{14}C and ^{210}Pb.

178

179 *Proxy analyses*

180 Plant macrofossil analysis was undertaken for all six cores at 1- to 2-cm resolution. For the four
181 cores characterised as low hummock and high lawn ecotones, where the plant records indicated
182 changes in hydrology, we also conducted testate amoeba analysis as we expected these changes
183 to be more reliably visible in testate amoeba records (Gałka, Tobolski, Górska & Lamentowicz,
184 2017; Väliranta et al., 2012; Zhang et al., 2018a). Testate amoeba analysis was first performed
185 at 4-cm resolution, but in cases where prominent changes occurred, the resolution was increased
186 to 2-cm. The lower resolution was sufficient where the proxy-based WTD reconstruction was
187 used as an environmental variable in explaining carbon accumulation patterns, as carbon
188 accumulation rate calculations were completed at 4-cm resolution and were therefore
189 comparable with the testate amoeba results.

190 Plant macrofossil analysis was performed following Väliranta et al. (2007). Volumetric samples
191 (*c*. 5 cm^3) were gently rinsed under running water using a 140-µm sieve. No chemical treatment
192 was applied. Remains retained on the sieve were identified. Proportions of different plant types
193 and unidentifiable organic matter (UOM) were estimated with the aid of a scale paper under a
194 petri dish using a stereomicroscope at the magnification of 10 – 40. Further identification to
195 species level was carried out using a high-power light microscope at the magnification of 100
196 – 200. Plant-based WTD reconstruction was carried out using the modern vegetation survey
197 data from the Siikaneva and Lakkasuo sites based on a weighted average approach; transfer
198 function development followed the methods described in Zhang et al. (2017).

199 Processing of testate amoeba samples followed a modified version of the standard method
200 (Booth, Lamentowicz & Charman, 2010). Samples were boiled in distilled water for 15 min
201 and stirred occasionally. The samples were then sieved with a 300-μm mesh and back sieved
202 with a 15-μm mesh. Materials retained on the 15-μm sieve were centrifuged at 3000 r.p.m. for
203 5 min. At least 100 individual shells for each sample were counted and identified to species or
204 "type" level under a light microscope at the magnification of 200 – 400. Taxonomy followed
205 Charman et al. (2000), supplemented with online sources (Siemensma, 2019). Testate amoeba-
206 based WTD reconstructions were performed using the transfer function developed by
207 Amesbury et al. (2016). Absolute WTD values (the larger the values the drier the conditions)
208 were normalized to z scores over the length of each core (Swindles et al., 2015). $Z > 0$ indicates
209 drier conditions than the sequence's average, $z < 0$ indicates conditions wetter than average.
210 We calculated the total proportion of mixotrophic testate amoeba taxa (here *Amphitrema*
211 *wrightianum*, *Archerella flavum*, *Heleopera sphagni*, *Hyalosphenia papilio*, *Placocista spinosa*)
212 that contribute to carbon cycling in peatlands (Jassey et al., 2015).

213 A LOESS smoothing function with a span-value (degree of smoothing) setting of 0.5 was
214 applied to the compiled proxy-wise WTD (z scores) dataset to explore the overall hydrological
215 changes reflected on different proxies. The analysis was completed using the function loess ()
216 in R version 3.6.0.

217

218 *Peat property analyses and carbon accumulation*

219 Contiguous samples of known volume (5 cm^3) were extracted from the cores at 1-cm resolution

and freeze-dried. Samples were then weighed to enable calculation of bulk density (g cm^{-3}), which was done by dividing the dry peat weight (g) by the wet peat volume (cm^3). Percentage of carbon and nitrogen content by mass was measured at every 4 cm on homogenously ground sub-samples using a Micro Cube Elemental Vario CNS-analyzer at the University of Helsinki, Finland. Carbon-to-nitrogen mass ratios (C/N) were calculated from C and N content data.

Vertical growth rates for each peat core were calculated based on the mean age estimates derived from the age-depth models. Apparent carbon accumulation rate (ACAR; g C m^{-2} yr^{-1}) was calculated by multiplying the bulk density of a depth-specific increment by its C content and by the accumulation rate. Peat decay modelling (Clymo, 1984) was used to derive the allogenic impacts-forced carbon accumulation variations (Zhang et al., 2018b). The Clymo model (1984) was first applied on the cumulative peat mass (bulk density) data to derive peat addition rate (*p*) and peat decay coefficient (α) using the curve fitting method. After which the derived parameters *p*, α and carbon content were used to calculate carbon accumulation rate (CAR) under constant conditions (autogenic accumulation). The difference (presented as CAR z scores) between ACAR and CAR are therefore interpreted to be driven by allogenic forcing.

Environmental drivers on carbon accumulation

To address the environmental controls on carbon accumulation patterns, linear regression analysis (95% confidence intervals

displayed) was applied to carbon accumulation rates and potential environmental variables. The environmental variables included reconstructed WTD z scores from testate amoebae for cores SLH, SHL, LLH and LHL, and from plant macrofossils for cores SLL and LLL; measured July-August temperature (thereafter referred to as summer temperature) data (1829-2016) from the Finnish Meteorological Institute; mixotrophic testate amoeba proportion for SLH, SHL, LLH and LHL. The analyses were first applied for individual cores and when this suggested that cores from the same habitat had similar patterns, habitat-specific analyses were performed and used for further discussions. The analysis was carried out using the lm() function in R version 3.6.0.

Results

Chronology and vertical peat growth

The studied peat cores from Siikaneva were dated to *c*. 1700–1820 AD, while Lakkasuo peat cores yielded basal ages of *c.* 1710–1760 AD. The ^{14}C dating of the basal sample from core SHL yielded a modern age and was detected as an outlier in the age-depth model. *Plum* uses a gamma autoregressive model to construct the chronology, this model gathers information from all the measurements and uses it to infer an age estimate at any depth (even when the measurements are not present). In the case of SHL, *Plum* used the information from the first 40

cm, where ^{210}Pb was measured, to infer a trend and memory parameters which allowed the model to conclude that the ^{14}C date was an outlier and then provided an age estimate given the information provided by the ^{210}Pb data, although with a bigger uncertainty, therefore the chronology of the section below *c*. 40 cm should be interpreted with caution. Peat accumulation rates have been relatively consistent within Lakkasuo peatland during recent centuries, while larger variations within individual peat cores and between different cores occurred at Siikaneva site (Tables 1 and S1-3, Figure 2).

Past vegetation succession

The plant macrofossil assemblages recorded *in situ* vegetation dynamics over the past *c*. 200–300 years. In all the six cores, *Sphagnum* spp. were the dominant component, occasionally accompanied by other taxa such as *Eriophorum vaginatum*, *Mylia anomala* and *Ericaceae* spp. (Figure 3).

For the driest low hummock habitat, *S. fuscum* and *S. rubellum* dominated core SLH from *c.* 1710–1950 AD, after this *S. fuscum* was the only abundant taxon accompanied by *Eriophorum vaginatum* from *c.* 1980 to 2000 AD. Lakkasuo core LLH was first occupied by *S. balticum* and *S. magellanicum* during *c*. 1710–1770 AD, after which *S. fuscum* became abundant.

For the mid-range high lawn habitat, at Siikaneva *S. rubellum* was abundant throughout the whole section, with *S. balticum* present from *c.* 1820 to 2005 AD but *S. fuscum* was more commonly recorded after *c.* 1990 AD. For the Lakkasuo record, the bottom sample at *c*. 1730 AD was dominated by *S. magellanicum*. After that, *S. balticum* was abundant with the presence

283 of *S. majus/cuspidatum* and *S. angustifolium* until *c.* 1960 AD. Afterwards, until the present, *S.*
284 *balticum* was accompanied by *S. fuscum*.

285 For the wettest low lawn habitat, vegetation was more variable than for the other two habitat
286 types. At first, *c*. 1740–1800 AD, the Siikaneva assemblage was dominated by *S. papillosum*
287 and *S. rubellum*, but then dominated by *S. cuspidatum* characteristic to wet hollows. Later the
288 habitat changed back to *S. papillosum*-dominated drier lawn (*c.* 1850 to 1970 AD), followed by
289 *S. rubellum*-dominated assemblage towards more recent times. The Lakkasuo assemblage was
290 initially occupied by *S. magellanicum* and *S. balticum* between *c*. 1810 and 1850 AD, followed
291 by *S. cuspidatum/majus* and *S. balticum*-dominated assemblages. Starting from *c*. 1890 AD, *S.*
292 *rubellum* became abundant.

293

294 *Reconstructed water-table depth (WTD)*

295 The plant macrofossil-based WTD transfer function had a good performance (R^2 = 0.80,
296 RMSEP = 4.35 cm). Model-derived tolerances around WTD optima were very narrow (1 to 3
297 cm) for species in wet habitats where water level is close to or at the moss surface, while species
298 adapted to drier habitats had larger tolerances, up to 12 cm (Figure S1).

299 In total, 40 testate amoeba taxa were detected from the four cores (Figure 3) that were used for
300 reconstructing WTD. *Archerella flavum* was dominant in all the cores, with also *Difflugia pulex*
301 in the cores SLH, SHL and LLH, *Hyalosphenia elegans* in cores SHL and SLH, and *Alabasta*
302 *militaris* type in core SLH.

303 In core SLH, plant-based WTD showed only little variability, the range being within *c.* 5 cm,

but testate amoeba-based WTD showed more conspicuous variations, especially for the period around *c.* 1840 AD in the late LIA where there is a remarkable wet to dry change (*c*. 10 cm) (Figure 3). For core LLH, both proxies showed comparable WTD patterns, i.e. from wet conditions before *c.* 1790 AD to dry conditions afterwards. The SHL testate amoeba record suggests large moisture change towards wetter habitat conditions dated to *c.* 1940–1950 AD but the plant-based WTD remained relatively stable; the assemblages were dominated by *S. rubellum* with a large tolerance of 8 cm (Figure S1). For LHL, both reconstructions suggest a wet phase between *c.* 1730 and 1830 AD and a dry period after *c.* 1960 AD. For the period between them, *c.* 1830-1960 AD, plant-WTD shows more variations than testate amoeba-based WTD, but both suggest medium dry conditions compared with the other two phases. For the SLL record, no large hydrological changes were detected; the general conditions remained wet. While the overall conditions at LLL were drier than SLL, especially after *c.* 1950 AD when the water table went down, several more recent wet periods were captured.

In general, plant- and testate amoeba-based WTD reconstructions support each other, while the latter tends to have more and/or larger variations, as also suggested by previous studies (Gałka et al., 2017; Väliranta et al., 2012; Zhang et al., 2018a). Therefore, we used testate amoeba-based WTD reconstructions for linear regression analysis when available, i.e. for all the other cores except low lawns where only plant-based WTD reconstructions existed.

Carbon accumulation and associations with environmental variables

Peat properties varied with depth and between different records (Table 1). For all the studied records, bulk density was 0.05 ± 0.01 (mean ± SD) g cm^{-3}, carbon content was 43.01 ± 2.34%, while nitrogen content was 0.71 ± 0.28%. Apparent carbon accumulation rates (ACAR) varied considerably (72.15 ± 69.75 g C m^{-2} yr^{-1}). All the studied sections showed a rapid increase of ACAR for the recent years (after 2000 AD) except the core LLL, which had relatively consistent ACARs throughout (Figure 3).

Although CAR z scores (allogenic forcing-driven carbon accumulation rate variations) indicate some core-specific features, the general pattern suggests that for low hummocks, high lawns and Siikaneva low lawn the environmental changes have promoted carbon accumulation (i.e. z > 0) before *c*. 1830–1850 AD and after 1980 to 2000 AD (Figure 3). But for Lakkasuo low lawn, its CAR z scores only increased between the period from 1950 to 1990 AD.

For low hummocks there were significant correlations between all the studied environmental variables and allogenic carbon accumulation variations measured as CAR z scores (Figure 4). In contrast, correlations were not found for the two other habitats: high lawns and low lawns (Figure S2). For low hummocks, a significant negative correlation ($R^2 = 0.5031$, $p < 0.001$) was detected between CAR z scores and WTD (Figure 4a), meaning lower carbon accumulation in drier conditions. The correlation between CAR z scores and summer temperature was positive ($R^2 = 0.3184$, $p < 0.01$) (Figure 4b), but the correlation was weaker than between CAR z scores and WTD. Abundance of mixotrophic testate amoebae were positively linked to carbon accumulation ($R^2 = 0.4207$, $p < 0.001$) (Figure 4c). A further investigation of the distribution

of mixotrophic testate amoebae in different habitats indicated that in low hummocks, the abundance of mixotrophic testate amoebae was strongly linked to WTD (Figure S3; $R^2 = 0.7608$, $p < 0.001$). However, in high lawns, this link was weaker, but still significant ($R^2 = 0.3006$, $p < 0.001$).

Discussion

Climate-driven centennial-scale bog surface drying

We detected a consistent peatland surface drying, inferred from both proxies (Figures 3 and 5). In general, testate amoeba records suggest a gradual drying since the 1800s, most clearly visible in low hummocks and in the Lakkasuo high lawn core, while shifts in vegetation towards plant communities adapted to drier microhabitat occurred either synchronously or a few decades later. This drying trend is in line with another record from southern Finland, where *Sphagnum rubellum* and *S. balticum* communities were replaced by a *S. fuscum*-dominated community at around 1800 AD (Väliranta et al., 2007). At low hummocks and high lawns, the vegetation change was reflected as a replacement of wet lawn *Sphagna* by dry hummock *Sphagna*, such as *S. fuscum*. For low lawns, the changes were more gradual from wet hollow taxa to lawn or even hummock taxa. Some previous studies have suggested that increase in *S. fuscum* abundancy might result from increased atmospheric nitrogen input (Vitt, Wieder, Halsey, & Turetsky, 2003; Wieder et al., 2016). However, the geochemical analyses did not indicate any increased nitrogen load on our peatlands. In addition, a previous study found that compared to, for example, central Europe, Finland still has a markedly small nitrogen load (Dirnböck et al.,

368 2014). Therefore, our data suggest the changes in plant communities were mainly driven by
369 changes in (climate driven) hydrology.

370 Our results imply that changes in hydrology were related to changes in temperature and
371 precipitation. Most of the vegetation shifts towards drier communities occurred after the Little
372 Ice Age, which ended *c*. 1850 AD. However, we also recorded dry shifts during the latter part
373 of the LIA, as also inferred by the testate amoeba assemblages. For example, at both study sites
374 a notable shift in vegetation towards dry communities occurred *c.* 1770 AD. No measured
375 meteorological data exist for that period, but solar irradiance reconstructions have suggested
376 that around 1770 AD the irradiation level was as high as that of around 1930–1940 AD (Lean,
377 Beer, & Bradley, 1995), when measured temperatures were high. This suggests that summer
378 temperature seems to play a critical role in controlling bog vegetation communities via changes
379 in moisture conditions. Measured summer temperature records warmer than 17.3 °C (average
380 for the period 1990-2018) corresponded with each of the other drying phases. In particular, in
381 the 1940s AD several continuous warm summers followed one another, and these may have
382 contributed to the substantial successional change towards drier vegetation that we recorded.
383 The detected link between *Sphagnum* community changes and summer temperature is in line
384 with studies from Alberta, Canada, where the increase in summer temperature and consequent
385 enhanced evapotranspiration resulted in a dry shift that triggered a vegetation change towards
386 *S. fuscum* domination (Magnan et al., 2018).

387 In addition to summer temperature, summer (June-August) precipitation might be another
388 factor that controls bog moisture changes. Even though instrumental climate records showed
389 that summer precipitation since 1850 AD had been annually variable with a range of *c*. 35 to

345 mm (mean ± SD: 200 ± 65 mm) and no clear trend, most of the drying vegetation shifts occurred during very dry summers (summer precipitation <100 mm). However, the same vegetation shifts also happened during wet summers (>250 mm) in the past decade, for example in SHL with increased proportion of *S. fuscum* and disappearing of *S. balticum*, which may result from increased evapotranspiration during warm summers. These recent wet summers might also explain the clear wet shifts recorded in low hummock testate amoeba data (SLH and LLH) *c.* 2000 AD, which indicate a higher sensitivity of testate amoebae to environmental changes than plants, as there were no clear corresponding vegetation changes towards wetter communities (Väliranta et al., 2012; Zhang et al., 2018a). However, it should also be noted that despite these recent wet shifts, conditions were still drier than the very early wet conditions during mid-late 1700s at both sites (Figure 5).

Response of carbon accumulation to climate forcing

Peatland carbon accumulation is mainly controlled by vegetation composition, water table and temperature. However, due to the complexity of interactions between these factors and the highly heterogeneous nature of peatlands, links between peat carbon accumulation and any individual environmental variables are not straightforward (e.g., Loisel and Garneau, 2010; Piilo et al., 2019; Zhang et al., 2018b). We did not observe any changes in plant functional types, e.g., from *Sphagnum* to shrubs (Tuittila et al., 2012), thus we assume that the detected variation in carbon accumulation rate is largely due to variations in moisture and temperature, although changes in moss community might alone could still drive changes in carbon

411 accumulation due to different photosynthesis and decomposition rates at the species level
412 (Hajek, Tuittila, Ilomets, & Laiho, 2009; Kangas et al., 2014; Laine, Juurola, Hajek, & Tuittila,
413 2011; Turetsky, Crow, Evans, Vitt, & Wieder, 2008).

414 Our results suggest that the response of carbon accumulation rate to environmental changes in
415 the past varied for different habitats. For low hummocks the CAR z scores showed significant
416 linear correlations to all studied variables. In contrast, the other two habitats, high lawns and
417 low lawns yielded no significant correlations. At low hummock conditions, summer
418 temperature showed a weak linear accelerating impact ($R^2 = 0.3184$, $p < 0.01$) on carbon
419 accumulation, while WTD showed a much stronger forcing ($R^2 = 0.5031$, $p < 0.001$), with drier
420 conditions resulting in lower carbon accumulation rates. Recent experimental studies support
421 our palaeo interpretation, by suggesting that WTD is a more important forcing factor than
422 temperature alone (Laine et al., 2019; Mäkiranta et al., 2018). The different response patterns
423 of the three habitats indicate that only in low hummock habitats WTD was a limiting factor for
424 carbon accumulation, whereas for lawns, water tables were sustained high enough to enable
425 effective carbon accumulation. The influence of the limiting factor WTD on carbon
426 accumulation likely worked through changes in biological communities, for example, the
427 decreased carbon accumulation under water-limited low hummocks can be partly linked to the
428 distinct decrease of mixotrophic testate amoeba abundance in such habitats ($R^2 = 0.7608$, $p <$
429 0.001), which can significantly cause reduced carbon accumulation ($R^2 = 0.4207$, $p < 0.001$)
430 (see also Jassey et al., 2015).

431

Carbon uptake capacity of boreal peatlands in the future

Our results suggest that in addition to global-scale impacts of warming on peatland carbon accumulation (Gallego-Sala et al., 2018), local small-scale hydrological conditions are crucial in controlling carbon accumulation dynamics. Thus, including moisture as a predictor variable for the future estimates of carbon dynamics is highly important. If we are to experience severe droughts and consequent water level drawdowns, peatland carbon uptake capacity is threatened. According to our study, Siikaneva where roughly 21% of the peatland area is covered by hummocks (Korrensalo et al., 2018) has, to some extent, already decreased carbon accumulation capacity due to surface drying since 1850 AD – the most severe periods occurring from the 1850's to the late 1900's. If drying continues, most of the current lawn surfaces, which now cover *c*. 38% of the Siikaneva peatland area (Korrensalo et al., 2018), have the potential to turn to low hummock habitats; this development has already been predicted in a field experimental study at Lakkasuo (Kokkonen et al., 2019). This potential habitat transition will also stress mixotrophic testate amoebae, as current lawn conditions are generally more appropriate habitats for most of the mixotrophic testate amoeba taxa (e.g., Zhang et al., 2018c). Therefore, further drying may reduce the abundance of mixotrophic testate amoebae and consequently reduce peatland C fixation. This scenario is in line with a recent model-based pan-Arctic carbon accumulation prediction study that shows decreased carbon accumulation for southern Finland by the end of 21st century in comparison to the accumulation rate in the 20th century (Chaudhary, Miller, & Smith, 2017). Widespread drying of boreal peatlands in recent centuries has been very recently recorded (Swindles et al., 2019; van Bellen et al., 2018). The future climate prediction for Fennoscandia is warmer and wetter (CMIP5 under RCP8.5)

(Collins et al., 2013). However, and more importantly, a net effect on summer moisture balance may be negative, as increased evapotranspiration may result in summer-time moisture deficit. Bogs are suggested to be more resistant to drying than fens (Jaatinen, Fritze, Laine, & Laiho, 2007; Kokkonen et al., 2019), as they already regularly experience dry seasons/periods (Thormann, Bayley, & Szumigalski, 1998). Yet, here we evidenced consistent climate-driven water level variations, dry shifts and subsequent changes in biological assemblages in two adjacent bogs under warmer conditions in the past. With prolonged warming and consequent peat surface drying, *Sphagna* communities may be even gradually replaced by shrubs (McPartland et al., 2019; Munir, Xu, Perkins, & Strack, 2014), which would have more profound impacts on peatland carbon uptake capacity (Loisel et al., 2014; Munir et al., 2014).

In summary, the two studied southern boreal bogs with separate catchment areas consistently showed shifts towards drier peatland surface conditions during recent centuries. The general drying trend was reflected in both plant and testate amoeba communities. Both summer temperature and precipitation, and more importantly effective moisture balance, are important drivers of peatland vegetation and hydrological conditions. Our study suggests that environmental forcing on carbon accumulation is most prominent for low hummock habitats. In short, the drier the conditions, the less carbon accumulated. The above derived patterns reveal that even though peatland carbon accumulation processes are complex, they will become more predictable when some controlling factors reach their threshold levels. We preliminarily conclude that carbon sink capacity of northern bogs is endangered if the future climate warming results in bog moisture deficiency. Peat surface drying might lead to eventual proportional decrease of lawn areas and increase the area of hummocks, although the possibly correspondent

476 decrease of hollow areas might on the other hand mitigate the carbon accumulation reduction
477 by reducing methane emissions.

478

479 **Acknowledgements**

480 This work was supported by Academy of Finland project 287039. We thank Joonas Alanko and
481 Miika Huilla for laboratory and plant macrofossil analyses, Nicola Kokkonen and Aino
482 Korrensalo for modern vegetation surveys and assistance in the field sampling. We thank the
483 reviewers for their constructive comments. The authors declare there is no conflict of interest.

484

485 **Data availability**

486 The data that support the findings of this study are available from the corresponding author
487 upon reasonable request.

488

489 **References**

490 Amesbury, M. J., Swindles, G. T., Bobrov, A., Charman, D. J., Holden, J., Lamentowicz, M., .
491 . . Warner, B. G. (2016). Development of a new pan-European testate amoeba transfer
492 function for reconstructing peatland palaeohydrology. *Quaternary Science Reviews,*
493 *152*, 132-151. doi:10.1016/j.quascirev.2016.09.024
494 Andersen, R., Poulin, M., Borcard, D., Laiho, R., Laine, J., Vasander, H., & Tuittila, E.-T.
495 (2011). Environmental control and spatial structures in peatland vegetation. *Journal of*
496 *Vegetation Science, 22*(5), 878-890. doi:10.1111/j.1654-1103.2011.01295.x
497 Aquino-López, M. A., Blaauw, M., Christen, J. A., Sanderson, N. K. (2018). Bayesian analysis
498 of ^{210}Pb dating. *Journal of Agricultural, Biological and Environmental Statistics*, 23,
499 317-333. doi:10.1007/s13253-018-0328-7
500 Arnaud, F., Magand, O., Chapron, E., Bertrand, S., Boës, X., Charlet, F. & Mélières, M.-
501 A. (2006). Radionuclide dating (^{210}Pb, ^{137}Cs, ^{241}Am) of recent lake sediments in a
502 highly active geodynamic setting (Lakes Puyehue and Icalma—Chilean Lake District).
503 *Science of The Total Environment*, *366*, 837-850. doi:10.1016/j.scitotenv.2005.08.013
504 Booth, R.K., Lamentowicz, M., & Charman, D. J. (2010). Preparation and analysis of testate
505 amoebae in peatland palaeoenvironmental studies. *Mires and Peat*, *7*, Article 2.
506 Retrieved from http://www.mires-and-peat.net/pages/volumes/map07/map0702.php
507 Brock, F., Higham, T., Ditchfield, P. & Ramsey, C. (2010). Current pretreatment methods for
508 AMS radiocarbon dating at the Oxford Radiocarbon Accelerator Unit (ORAU).

Radiocarbon, 52, 103-112. doi:10.1017/S0033822200045069

Charman, D. J., Hendon, D., & Woodland, W. A. (2000). The identification of testate amoebae (Protozoa: Rhizopoda) in peats. *Quaternary Research Association, Oxford.*

Chaudhary, N., Miller, P. A., & Smith, B. (2017). Modelling past, present and future peatland carbon accumulation across the pan-Arctic region. *Biogeosciences, 14*(18), 4023-4044. doi:10.5194/bg-14-4023-2017

Clymo, R.S. (1984). The limits to peat bog growth. *Philosophical Transactions of Royal Society Lond B, 303*, 605-654.

Collins, M., R. Knutti, J. Arblaster, J.-L. Dufresne, T. Fichefet, P. F., X. Gao, . . . M. Wehner. (2013). Long-term climate change: projections, commitments and irreversibility. In: Climate Change 2013: The physical science basis. Contribution of working group I to the fifth assessment report of the Intergovernmental Panel on Climate Change [Stocker, T.F., D. Qin, G.-K. Plattner, M. Tignor, S.K. Allen, J. Boschung, A. Nauels, Y. Xia, V. Bex and P.M. Midgley (eds.)]. Cambridge University Press, Cambridge, United Kingdom and New York, NY, USA.

De Vleeschouwer, F., Chambers, F. M., & Swindles, G. T. (2010). Coring and sub-sampling of peatlands for palaeoenvironmental research. *Mires and Peat, 7*. Article 1. Retrieved from http://www.mires-and-peat.net/pages/volumes/map07/map0701.php

Dieleman, C. M., Branfireun, B. A., McLaughlin, J. W., & Lindo, Z. (2015). Climate change drives a shift in peatland ecosystem plant community: Implications for ecosystem function and stability. *Global Change Biology, 21*(1), 388-395. doi:10.1111/gcb.12643

Dirnböck, T., Grandin, U., Bernhardt-Römermann, M., Beudert, B., Canullo, R., Forsius, M., . . .Uziębło, A.K. (2014). Forest floor vegetation response to nitrogen deposition in Europe. *Global Change Biology, 20*, 429-440. doi:10.1111/gcb.12440

Estop-Aragonés, C., Cooper, M. D. A., Fisher, J. P., Thierry, A., Garnett, M. H., Charman, D. J., . . . Hartley, I. P. (2018). Limited release of previously-frozen C and increased new peat formation after thaw in permafrost peatlands. *Soil Biology and Biochemistry, 118*, 115-129. doi:10.1016/j.soilbio.2017.12.010

Frolking, S., Roulet, N. T., Tuittila, E., Bubier, J. L., Quillet, A., Talbot, J., & Richard, P. J. H. (2010). A new model of Holocene peatland net primary production, decomposition, water balance, and peat accumulation. *Earth System Dynamics, 1*(1), 1-21. doi:10.5194/esd-1-1-2010

Gałka, M., Tobolski, K., Górska, A., & Lamentowicz, M. (2017). Resilience of plant and testate amoeba communities after climatic and anthropogenic disturbances in a Baltiv bog in Northern Poland: Implications for ecological restoration. *The Holocene, 27*(1), 130-141. doi: 10.1177/0959683616652704

Gallego-Sala, A. V., Charman, D. J., Brewer, S., Page, S. E., Prentice, I. C., Friedlingstein, P., . . . Zhao, Y. (2018). Latitudinal limits to the predicted increase of the peatland carbon sink with warming. *Nature Climate Cha*nge, 8, 907-913. doi:10.1038/s41558-018-0271-1

Gilbert, D., Amblard, C., Bourdier, G., & Francez, A.-J. (1998). The microbial loop at the surface of a peatland: Structure, function, and impact of nutrient input. *Microbial Ecology, 35*, 83-93. doi:10.1007/s002489900062

552 Hajek, T., Tuittila, E.-S., Ilomets, M., & Laiho, R. (2009). Light responses of mire mosses – a
553 key to survival after water-level drawdown? *Oikos, 118*(2), 240-250.
554 doi:10.1111/j.1600-0706.2008.16528.x
555 Helama, S., Meriläinen, J., & Tuomenvirta, H. (2009). Multicentennial megadrought in
556 northern Europe coincided with a global EI Niño - Southern Oscillation drought pattern
557 during the Medieval Climate Anomaly. *Geology, 37*(2), 175-178.
558 doi:10.1130/G25329A.1
559 Helama, S., Vartiainen, M., Holopainen, J., Mäkelä, H. M., Kolström, T., & Meriläinen, J.
560 (2014). A palaeotemperature record for the Finnish lakeland based on
561 microdensitometric variations in tree rings. *Geochronometria, 41*(3), 265-277.
562 doi:10.2478/s13386-013-0163-0
563 Holmquist, J.R., Finkelstein, S.A., Garneau, M., Massa, C., Yu, Z., & MacDonald, G.M. (2017).
564 A comparison of radiocarbon ages derived from bulk peat and selected plant
565 macrofossils in basal peat cores from circum-artic peatlands. *Quaternary*
566 *Geochronology, 31*, 53-61. doi:10.1016/j.quageo.2015.10.003
567 Jaatinen, K., Fritze, H., Laine, J., & Laiho, R. (2007). Effects of short- and long-term water-
568 level drawdown on the populations and activity of aerobic decomposers in a boreal
569 peatland. *Global Change Biology, 13*(2), 491-510. doi:10.1111/j.1365-
570 2486.2006.01312.x
571 Jassey, V. E., Signarbieux, C., Hattenschwiler, S., Bragazza, L., Buttler, A., Delarue, F., . . .
572 Robroek, B. J. (2015). An unexpected role for mixotrophs in the response of peatland
573 carbon cycling to climate warming. *Scientific Reports, 5,* doi:10.1038/srep16931
574 Jauhiainen, S., Holopainen, M., & Rasinmäki, A. (2007). Monitoring peatland vegetation by
575 means of digitized aerial photographs. *Scandinavian Journal of Forest Research, 22*(2),
576 168-177. doi:10.1080/02827580701217620
577 Jeter, H.W. (2000). Determining the ages of recent sediments using measurements of trace
578 radioactivity. *Terra et Aqua*, 78, 21-28.
579 Kangas, L., Maanavilja, L., Hajek, T., Juurola, E., Chimner, R. A., Mehtatalo, L., & Tuittila,
580 E.-S. (2014). Photosynthetic traits of *Sphagnum* and feather moss species in undrained,
581 drained and rewetted boreal spruce swamp forests. *Ecology and Evolution, 4*(4), 381-
582 396. doi:10.1002/ece3.939
583 Kelly, T. J., Lawson, I. T., Roucoux, K. H., Baker, T. R., Jones, T. D., & Sanderson, N. K.
584 (2017). The vegetation history of an Amazonian domed peatland. *Palaeogeography,*
585 *Palaeoclimatology, Palaeoecology, 468*, 129-141. doi:10.1016/j.palaeo.2016.11.039
586 Kokkonen, N., Laine, A., Laine, J., Vasander, H., Kurki, K., Gong, J., & Tuittila, E.-S. (2019).
587 Responses of peatland vegetation to 15-year water level drawdown as mediated by
588 fertility level. *Journal of Vegetation Science*. In press.
589 Korrensalo, A., Kettunen, L., Laiho, R., Alekseychik, P., Vesala, T., Mammarella, I., & Tuittila,
590 E.-S. (2018). Boreal bog plant communities along a water table gradient differ in their
591 standing biomass but not their biomass production. *Journal of Vegetation Science, 29*(2),
592 136-146. doi:10.1111/jvs.12602
593 Laine, A. M., Juurola, E., Hajek, T., & Tuittila, E.-S. (2011). *Sphagnum* growth and
594 ecophysiology during mire succession. *Oecologia, 167*(4), 1115-1125.

595 doi:10.1007/s00442-011-2039-4
596 Laine, A. M., Mäkiranta, P., Laiho, R., Mehtätalo, L., Penttilä, T., Korrensalo, A., . . . Tuittila,
597 E.-S. (2019). Warming impacts on boreal fen CO_2 exchange under wet and dry
598 conditions. *Global Change Biology, 25*(6), 1995-2008. doi:10.1111/gcb.14617
599 Lara, E., Gomaa, F. (2017). Symbiosis between testate amoebae and photosynthetic organisms.
600 In: Algal and cyanobacteria symbioses [Grube, M., Seckbach, J., and Muggia, L. (eds.)].
601 World Publishing Europe Ltd. London, United Kingdom. doi:10.1142/9781786
602 340580_0013
603 Lean, J., Beer, J., & Bradley, R. (1995). Reconstruction of solar irradiance since 1610 -
604 implications for climate change. *Geophysical Research Letters, 22*(23), 3195-3198. doi:
605 10.1029/95gl03093
606 Loisel, J., Gallego-Sala, A. V., & Yu, Z. (2012). Global-scale pattern of peatland *Sphagnum*
607 growth driven by photosynthetically active radiation and growing season length.
608 *Biogeosciences, 9*(7), 2737-2746. doi: 10.5194/bg-9-2737-2012
609 Loisel, J., Garneau, M. (2010). Late Holocene paleoecohydrology and carbon accumulation
610 estimates from two boreal peat bogs in eastern Canada: Potential and limits of multi-
611 proxy archives. *Palaeogeography, Palaeoclimatology, Palaeoecology, 291*, 493-533.
612 Loisel, J., Yu, Z. C., Beilman, D. W., Camill, P., Alm, J., Amesbury, M. J., . . . Zhou, W. J.
613 (2014). A database and synthesis of northern peatland soil properties and Holocene
614 carbon and nitrogen accumulation. *The Holocene*. doi:10.1177/0959683614538073
615 Luoto, T. P., & Helama, S. (2010). Palaeoclimatological and palaeolimnological records from
616 fossil midges and tree-rings: the role of the North Atlantic Oscillation in eastern Finland
617 through the Medieval Climate Anomaly and Little Ice Age. *Quaternary Science*
618 *Reviews, 29*(17-18), 2411-2423. doi:10.1016/j.quascirev.2010.06.015
619 Magnan, G., van Bellen, S., Davies, L., Froese, D., Garneau, M., Mullan-Boudreau, G., . . .
620 Shotyk, W. (2018). Impact of the Little Ice Age cooling and 20th century climate change
621 on peatland vegetation dynamics in central and northern Alberta using a multi-proxy
622 approach and high-resolution peat chronologies. *Quaternary Science Reviews, 185*,
623 230-243. doi:10.1016/j.quascirev.2018.01.015
624 Mäkiranta, P., Laiho, R., Mehtätalo, L., Strakova, P., Sormunen, J., Minkkinen, K., . . . Tuittila,
625 E.-S. (2018). Responses of phenology and biomass production of boreal fens to climate
626 warming under different water-table level regimes. *Global Change Biology, 24*(3), 944-
627 956. doi:10.1111/gcb.13934
628 McPartland, M. Y., Kane, E. S., Falkowski, M. J., Kolka, R., Turetsky, M. R., Palik, B., &
629 Montgomery, R. A. (2019). The response of boreal peatland community composition
630 and NDVI to hydrologic change, warming, and elevated carbon dioxide. *Global Change*
631 *Biology, 25*(1), 93-107. doi:10.1111/gcb.14465
632 Mikola, J., Virtanen, T., Linkosalmi, M., Vähä, E., Nyman, J., Postanogova, O., . . . Aurela, M.
633 (2018). Spatial variation and linkages of soil and vegetation in the Siberian Arctic
634 tundra–coupling field observations with remote sensing data. *Biogeosciences, 15*(9),
635 2781-2801. doi:10.5194/bg-15-2781-2018
636 Munir, T. M., Xu, B., Perkins, M., & Strack, M. (2014). Responses of carbon dioxide flux and
637 plant biomass to water table drawdown in a treed peatland in northern Alberta: a climate

change perspective. *Biogeosciences, 11*(3), 807-820. doi:10.5194/bg-11-807-2014

Piilo, S. R., Zhang, H., Garneau, M., Gallego-Sala, A., Amesbury, M., & Väliranta, M. (2019). Recent peat and carbon accumulation following the Little Ice Age in northwestern Québec, Canada. *Environmental Research Letters*, *14*(7), doi:10.1088/1748-9326/ab11ec

Pirinen, P., Simola, H., Aalto, J., Kaukoranta, J.-P., Karlsson, P., & Ruuhela, R. (2012). Finnish Meteorological Institute Reports. Tilastoja Suomen Ilmastosta 1981-2010 (Climatological Statistics of Finland 1981-2010), vol. 1.

R Core Team. (2019). R: A language and environment for statistical computing. R Foundation for Statistical Computing, Vienna, Austria.

Reimer, P. J., Bard, E., Bayliss, A., Beck, J. W., Blackwell, P. G., Ramsey, C. B., . . . van der Plicht, J. (2013). IntCal13 and marine13 radiocarbon age calibration curves 0-50,000 years cal BP. *Radiocarbon, 55*(4), 1869-1887. doi:10.2458/azu_js_rc.55.16947

Riutta, T., Laine, J., Aurela, M., Rinne, J., Vesala, T., Laurila, T., . . . Tuittila, E.-S. (2007). Spatial variation in plant community functions regulates carbon gas dynamics in a boreal fen ecosystem. *Tellus B: Chemical and Physical Meteorology, 59*(5), 838-852. doi:10.1111/j.1600-0889.2007.00302.x

Siemensma, F. J. (2019). Microworld, world of amoeboid organisms. World-wide electronic publication, Kortenhoef, the Netherlands. https://www.arcella.nl.

Strack, M., Waddington, J. M., Rochefort, L., & Tuittila, E.-S. (2006). Response of vegetation and net ecosystem carbon dioxide exchange at different peatland microforms following water table drawdown. *Journal of Geophysical Research: Biogeosciences, 111*(G2), doi:10.1029/2005jg000145

Swindles, G. T., Holden, J., Raby, C. L., Turner, T. E., Blundell, A., Charman, D. J., . . . Kløve, B. (2015). Testing peatland water-table depth transfer functions using high-resolution hydrological monitoring data. *Quaternary Science Reviews, 120*, 107-117. doi:10.1016/j.quascirev.2015.04.019

Swindles, G. T., Morris, P. J., Mullan, D. J., Payne, R. J., Roland, T. P., Amesbury, M. J., …Warner, B. (2019). Widespread drying of European peatlands in recent centuries. *Nature Geoscience, 12*, 922-928. doi:10.1038/s41561-019-0462-z

Tahvanainen, T. (2011). Abrupt ombrotrophication of a boreal aapa mire triggered by hydrological disturbance in the catchment. *Journal of Ecology*, *99*(2), 404-415. doi:10.1111/j.1365-2745.2010.01778.x

Thormann, M. N., Bayley, S. E., & Szumigalski, A. R. (1998). Effects of hydrologic changes on aboveground production and surface water chemistry in two boreal peatlands in Alberta: Implications for global warming. *Hydrobiologia*, *362*, 171-183. doi:10.1023/A:1003194803695

Tuittila, E.-S., Juutinen, S., Frolking, S., Väliranta, M., Laine, A.M., Miettine, A., … Merilä, P. (2012). Wetland chronosequence as a model of peatland development: Vegetation succession, peat and carbon accumulation. *The Holocene, 23*(1), 25-35. doi:10.1177/0959683612450197

Tuittila, E.-S., Väliranta, M., Laine, J., & Korhola, A. (2007). Quantifying patterns and controls of mire vegetation succession in a southern boreal bog in Finland using partial

ordinations. *Journal of Vegetation Science, 18*, 891-902.

Turetsky, M. R., Crow, S. E., Evans, R. J., Vitt, D. H., & Wieder, R. K. (2008). Trade-offs in resource allocation among moss species control decomposition in boreal peatlands. *Journal of Ecology, 96*(6), 1297-1305. doi:10.1111/j.1365-2745.2008.01438.x

Väliranta, M., Blundell, A., Charman, D. J., Karofeld, E., Korhola, A., Sillasoo, U., & Tuittila, E.-S. (2012). Reconstructing peatland water tables using transfer functions for plant macrofossils and testate amoebae: A methodological comparison. *Quaternary International, 268*, 34-43. doi:10.1016/j.quaint.2011.05.024

Väliranta, M., Korhola, A., Seppä, H., Tuittila, E.-S., Sarmaja-Korjonen, K., Laine, J., & Alm, J. (2007). High-resolution reconstruction of wetness dynamics in a southern boreal raised bog, Finland, during the late Holocene: a quantitative approach. *The Holocene, 17*(8), 1093-1107. doi:10.1177/0959683607082550

van Bellen, S., Magnan, G., Davies, L., Froese, D., Mullan-Boudreau, G., Zaccone, C., . . . Shotyk, W. (2018). Testate amoeba records indicate regional 20th-century lowering of water tables in ombrotrophic peatlands in central-northern Alberta, Canada. *Global Change Biology, 24*(7), 2758-2774. doi:10.1111/gcb.14143

Vitt, D. H., Wieder, K., Halsey, L. A., & Turetsky, M. (2003). Response of *Sphagnum fuscum* to nitrogen deposition: A case study of ombrogenous peatlands in Alberta, Canada. *Bryologist, 106*(2), 235-245. doi: 10.1639/0007-2745(2003)106[0235:Rosftn]2.0.Co;2

Ward, S. E., Ostle, N. J., Oakley, S., Quirk, H., Henrys, P. A., & Bardgett, R. D. (2013). Warming effects on greenhouse gas fluxes in peatlands are modulated by vegetation composition. *Ecology Letters, 16*(10), 1285-1293. doi:10.1111/ele.12167

Weltzin, J. F., Bridgham, S. D., Pastor, J., Chen, J., & Harth, C. (2003). Potential effects of warming and drying on peatland plant community composition. *Global Change Biology, 9*(2), 141-151. doi:10.1046/j.1365-2486.2003.00571.x

Wieder, R. K., Vile, M. A., Albright, C. M., Scott, K. D., Vitt, D. H., Quinn, J. C., & Burke-Scoll, M. (2016). Effects of altered atmospheric nutrient deposition from Alberta oil sands development on *Sphagnum fuscum* growth and C, N and S accumulation in peat. *Biogeochemistry, 129*(1-2), 1-19. doi:10.1007/s10533-016-0216-6

Wiedermann, M. M., Nordin, A., Gunnarsson, U., Nilsson, M. B., & Ericson, L. (2007). Global change shifts vegetation and plant-parasite interactions in a boreal mire. *Ecology, 88*(2), 454-464. doi:10.1890/05-1823

Wu, J., Kutzbach, L., Jager, D., Wille, C., & Wilmking, M. (2010). Evapotranspiration dynamics in a boreal peatland and its impact on the water and energy balance. *Journal of Geophysical Research, 115*, doi:10.1029/2009JG001075.

Zhang, H., Amesbury, M. J., Ronkainen, T., Charman, D. J., Gallego-Sala, A. V., & Väliranta, M. (2017). Testate amoeba as palaeohydrological indicators in the permafrost peatlands of north-east European Russia and Finnish Lapland. *Journal of Quaternary Science, 32*(7), 976-988. doi:10.1002/jqs.2970

Zhang, H., Gallego-Sala, A. V., Amesbury, M. J., Charman, D. J., Piilo, S. R., & Väliranta, M. (2018b). Inconsistent response of arctic permafrost peatland carbon accumulation to warm climate phases. *Global Biogeochemical Cycles, 32*(10), 1605-1620. doi:10.1029/2018gb005980

Zhang, H., Piilo, S. R., Amesbury, M. J., Charman, D. J., Gallego-Sala, A. V., & Väliranta, M. (2018a). The role of climate change in regulating Arctic permafrost peatland hydrological and vegetation change over the last millennium. *Quaternary Science Reviews, 182*, 121-130. doi:10.1016/j.quascirev.2018.01.003

Zhang, H., Väliranta, M., Amesbury, M. J., Charman, D. J., Laine, A., & Tuittila, E.-S. (2018c). Successional change of testate amoeba assemblages along a space-for-time sequence of peatland development. *European Journal of Protistology, 66*, 36-47. doi:10.1016/j.ejop.2018.07.003

Figure caption and table

FIGURE 1 Upper panel: Location of the two study sites (red stars), the base map was downloaded from the National Land Survey of Finland Topographic Database under a CC 4.0 open source license. Lower panel: (a and b) Aerial photos of Siikaneva and Lakkasuo peatlands (2019 Google), red arrows show the coring points; (c) The microtopography-specific sampling design.

FIGURE 2 Age-depth models of the studied cores developed using *Plum*. The measured unsupported ^{210}Pb activities are in green, ^{137}Cs activities (SLH) are in black and calibrated ^{14}C dates are in blue. The grey shading indicates the 95% confidence range of the age-model. The red line is the weighted mean age based on the model. The ^{137}Cs-peak indicated 1986 AD at depth 21-22 cm (in core SLH) is shown using a black star.

FIGURE 3 Diagrams showing selected peat property (i.e. BD: bulk density; C/N: carbon nitrogen mass ratio; C%: C content; ACAR: apparent carbon accumulation rate; CAR: allogenic carbon accumulation rate), plant macrofossil and testate amoeba percentages for the studied six cores. Mixotrophic testate amoeba taxa are marked in red. Plant macrofossil- and testate amoeba-based water-table depth (WTD) reconstructions are also shown. The timing of post-Little Ice Age warming (1850 AD) is indicated using a red line. Main vegetation drying shifts are marked using blue lines.

FIGURE 4 Linear regression analyses of allogenic carbon accumulation rate (CAR) z scores and environmental variables for low hummocks. Analyses for high lawns and low lawns are shown in Figure S2. (a) water-table depth (WTD); (b) summer temperature (T); (c) mixotrophic testate amoeba (TA) abundance. The gray shading areas represent the 95% confidence intervals.

FIGURE 5 Summary of testate amoeba (TA)- and plant-based water-table depth (WTD) reconstructions and peatland vegetation successions in the studied cores. Only selected plants

761 are shown for each core showing the main moisture changes using colour-based WTD
762 indications derived from Figure S1. Each drying vegetation change is indicated using a black
763 arrow. Mean summer temperature and total summer precipitation are shown with the means for
764 the periods before and after 2000 AD indicated using vertical lines.

765

766 **TABLE 1** Detailed description of studied peat cores. WTD: Water-table depth of the sampling
767 point. BD: bulk density. C%: carbon content. N%: nitrogen content. PAR: peat accumulation
768 rate.

Site	Core	WTD (cm)	Surface vegetation	Core depth (cm)	Basal age (cal yr AD)	BD (g cm^{-3})	C%	N%	PAR (cm yr^{-1})
Siikaneva	#*SLH	17	*Sphagnum fuscum*	57	1744 – 1644	0.06 ± 0.01	43.65±0.99	0.73±0.24	0.45±0.54
	*SHL	8	*S. rubellum*, *S. fuscum*	49	1770 – 1874	0.05 ± 0.01	44.28±2.78	0.58±0.15	0.63±0.57
	*SLL	3	*S. rubellum, S. papilosum*	52	1685 – 1741	0.05 ± 0.15	43.30±0.70	0.88±0.41	0.38±0.66
Lakkasuo	*LLH	10	*S. fuscum*	58	1683 – 1737	0.07 ± 0.01	43.37±3.17	0.73±0.29	0.27±0.21
	*LHL	6	*S. balticum, S. fuscum*	61	1684 – 1738	0.05 ± 0.01	40.91±0.42	0.60±0.13	0.27±0.19
	*LLL	3	*S. rubellum, S. balticum*	54	1731 – 1805	0.05 ± 0.01	42.87±2.69	0.74±0.23	0.23±0.07

769 *Note*. *: Surface age control was based on ^{210}Pb dating. #: Surface age control was validated by ^{137}Cs dating.
770 The basal ages were based on ^{14}C dating except core SHL, which was modelled by *Plum*.

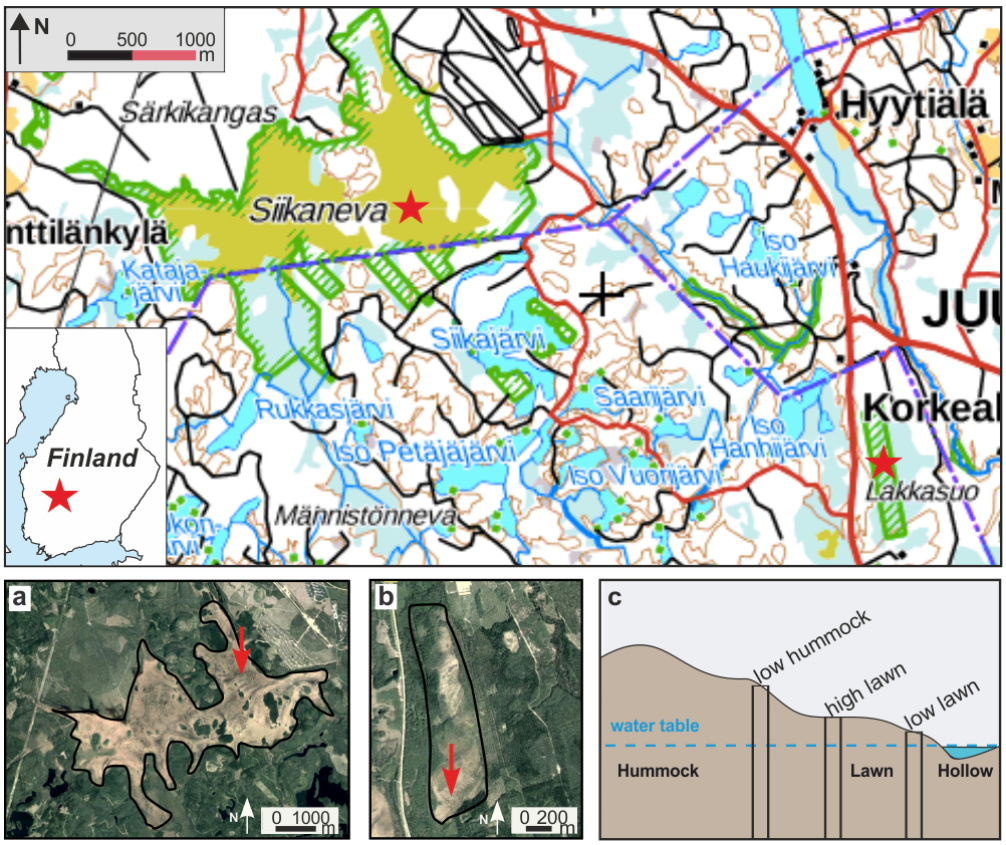

FIGURE 1 Upper panel: Location of the two study sites (red stars), the base map was downloaded from the National Land Survey of Finland Topographic Database under a CC 4.0 open source license. Lower panel: (a and b) Aerial photos of Siikaneva and Lakkasuo peatlands (2019 Google), red arrows show the coring points; (c) The microtopography-specific sampling design.

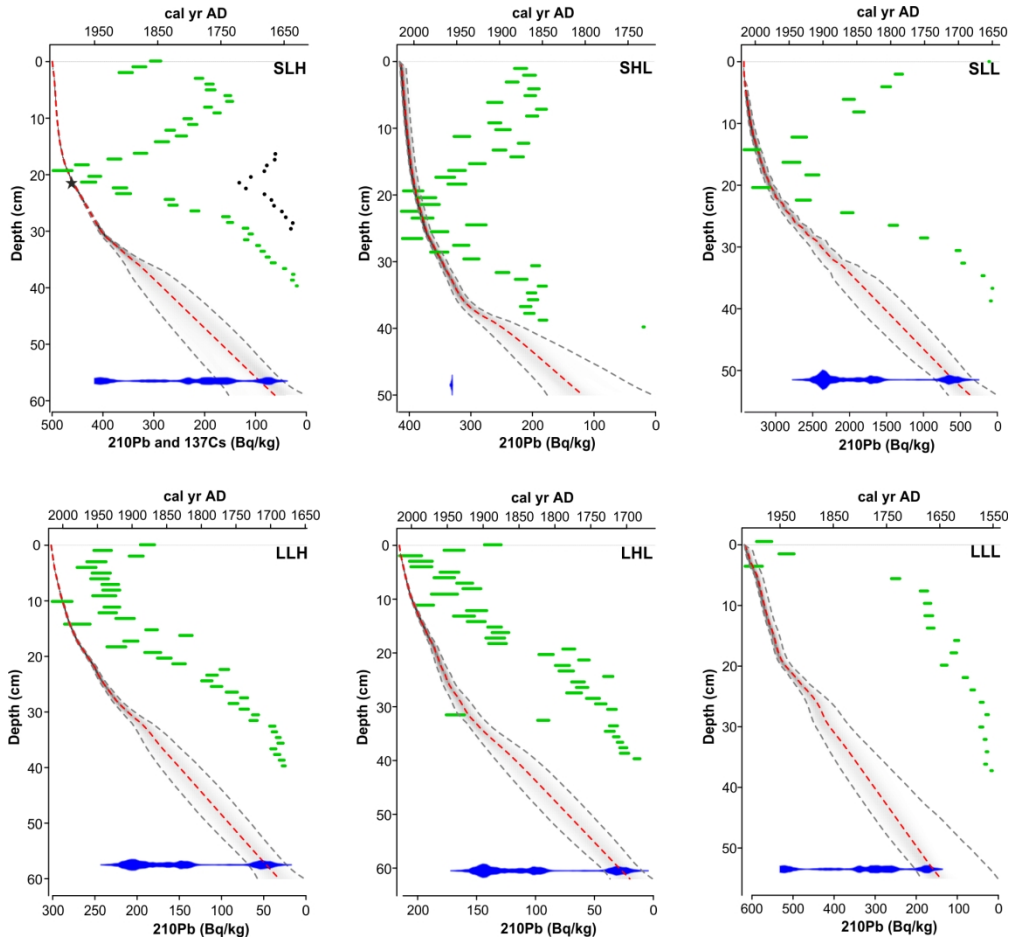

FIGURE 2 Age-depth models of the studied cores developed using Plum. The measured unsupported 210Pb activities are in green, 137Cs activities (SLH) are in black and calibrated 14C dates are in blue. The grey shading indicates the 95% confidence range of the age-model. The red line is the weighted mean age based on the model. The 137Cs-peak indicated 1986 AD at depth 21-22 cm (in core SLH) is shown using a black star.

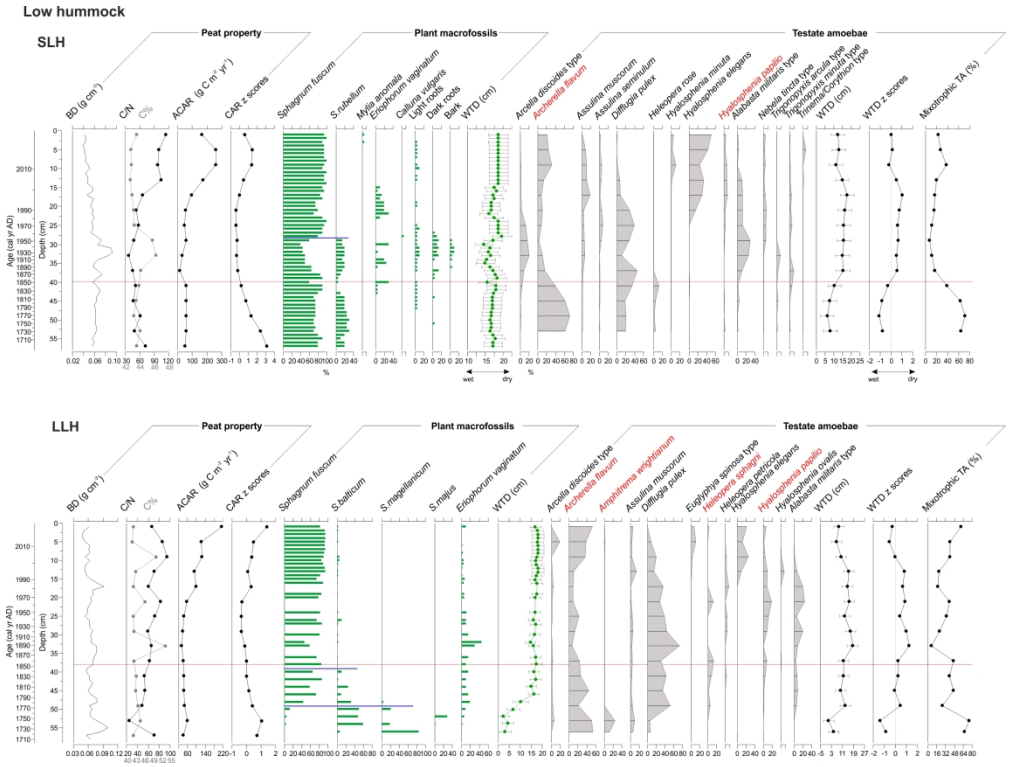

FIGURE 3 Diagrams showing selected peat property (i.e. BD: bulk density; C/N: carbon nitrogen mass ratio; C%: C content; ACAR: apparent carbon accumulation rate; CAR: allogenic carbon accumulation rate), plant macrofossil and testate amoeba percentages for the studied six cores. Mixotrophic testate amoeba taxa are marked in red. Plant macrofossil- and testate amoeba-based water-table depth (WTD) reconstructions are also shown. The timing of post-Little Ice Age warming (1850 AD) is indicated using a red line. Main vegetation drying shifts are marked using blue lines.

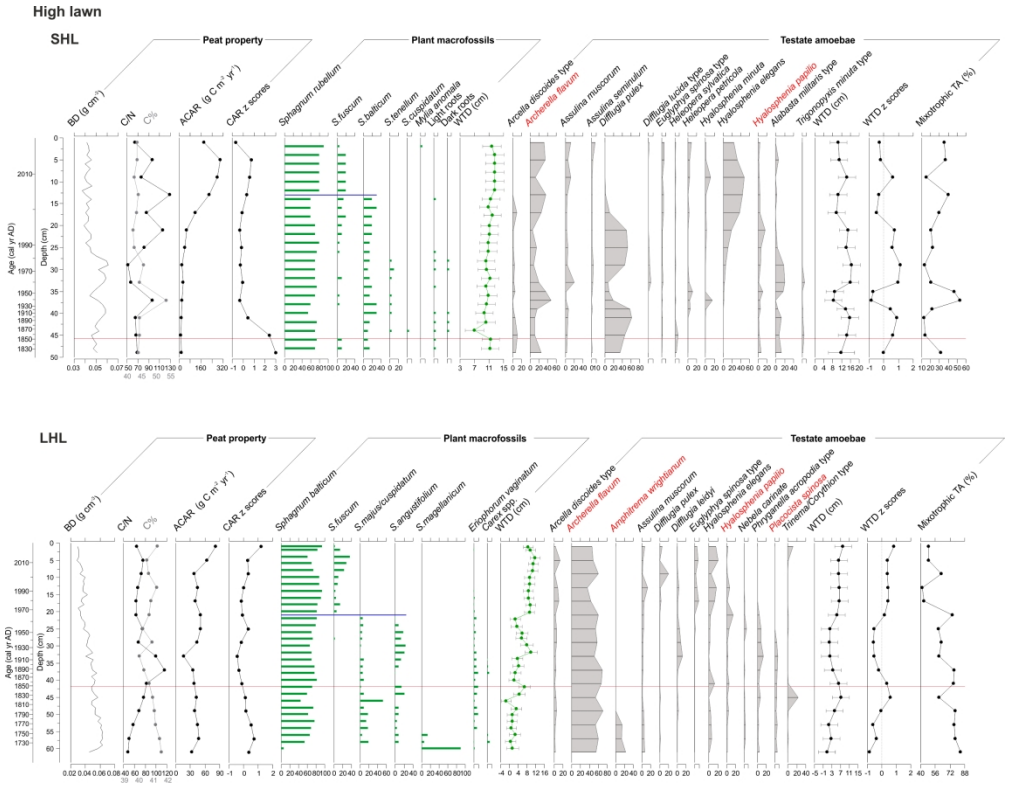
High lawn
SHL
Peat property
Plant macrofossils
Testate amoebae
BD (g cm-3)
C/N
C%
ACAR (g C m-2 yr-1)
CAR z scores
Sphagnum rubellum
S.fuscum
S.balticum
S.tenellum
S.cuspidatum
Myrica gramnale
Ledi rotata
Dark rocks
WTD (cm)
Arcella discoides type
Archerella flavum
Assulina muscorum
Assulina seminulum
Difflugia pulex
Difflugia lucida type
Euglypha scincsa type
Heleopera sylvatica
Heleopera petricola
Hyalosphenia minuta
Hyalosphenia elegans
Hyalosphenia papilio
Alabasta militaris type
Trigonopyxis minuta type
WTD (cm)
WTD z scores
Mixotrophic TA (%)
Age (cal yr AD)
Depth (cm)
LHL
Peat property
Plant macrofossils
Testate amoebae
BD (g cm-3)
C/N
C%
ACAR (g C m-2 yr-1)
CAR z scores
Sphagnum balticum
S.fuscum
S.majus/cuspidatum
S.angustifolium
S.magellanicum
Eriophorum vaginatum
Cane type
WTD (cm)
Arcella discoides type
Archerella flavum
Amphitrema wrightianum
Assulina muscorum
Difflugia pulex
Difflugia leidyi
Euglypha scincsa type
Hyalosphenia elegans
Hyalosphenia papilio
Nebela parvula
Physochila elongata
Phryganella acropodia type
Plagiopyxis sphroid
Trinema/Corythion type
WTD (cm)
WTD z scores
Mixotrophic TA (%)
Age (cal yr AD)
Depth (cm)

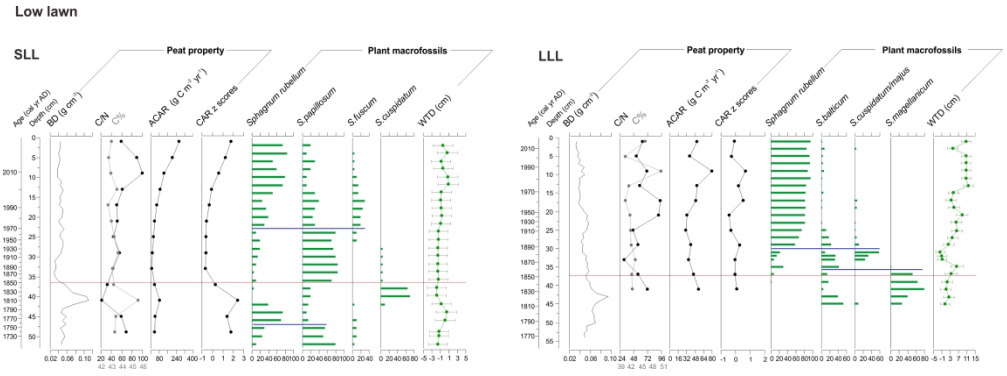
Low lawn
SLL
Peat property
Plant macrofossils
Age (cal yr AD)
Depth (cm)
BD (g cm-3)
C/N
C%
ACAR (g C m-2 yr-1)
CAR z scores
Sphagnum rubellum
S.papillosum
S.fuscum
S.cuspidatum
WTD (cm)
LLL
Peat property
Plant macrofossils
Age (cal yr AD)
Depth (cm)
BD (g cm-3)
C/N
C%
ACAR (g C m-2 yr-1)
CAR z scores
Sphagnum rubellum
S.balticum
S.cuspidatum/majus
S.magellanicum
WTD (cm)

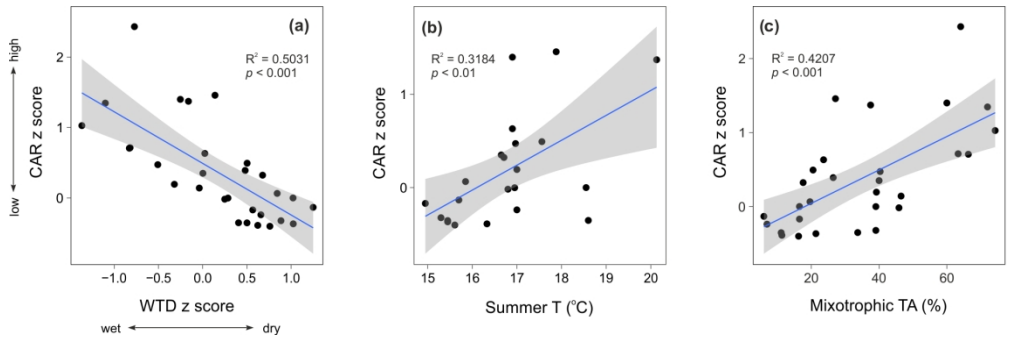

FIGURE 4 Linear regression analyses of allogenic carbon accumulation rate (CAR) z scores and environmental variables for low hummocks. Analyses for high lawns and low lawns are shown in Figure S2. (a) water-table depth (WTD); (b) summer temperature (T); (c) mixotrophic testate amoeba (TA) abundance. The gray shading areas represent the 95% confidence intervals.

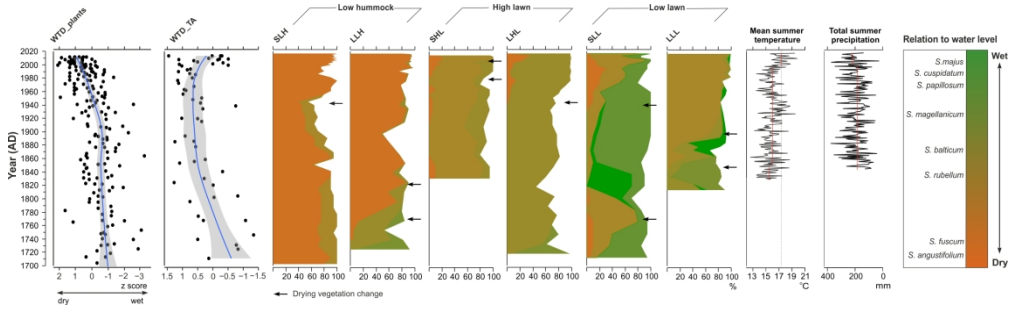

FIGURE 5 Summary of testate amoeba (TA)- and plant-based water-table depth (WTD) reconstructions and peatland vegetation successions in the studied cores. Only selected plants are shown for each core showing the main moisture changes using colour-based WTD indications derived from Figure S1. Each drying vegetation change is indicated using a black arrow. Mean summer temperature and total summer precipitation are shown with the means for the periods before and after 2000 AD indicated using vertical lines.